

AD-A056 091

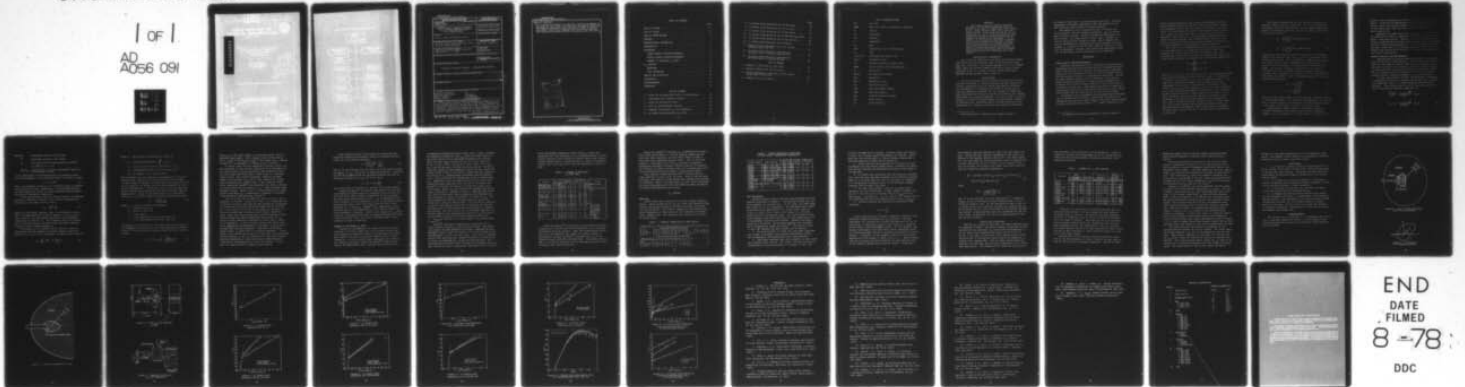
DAVID W TAYLOR NAVAL SHIP RESEARCH AND DEVELOPMENT CE--ETC F/G 11/6
ELASTIC-PLASTIC FRACTURE TOUGHNESS (J SUB IC) OF HIGH-STRENGTH --ETC(U)
JUN 78 J P GUDAS, J A JOYCE

UNCLASSIFIED

DTNSRDC-78/054

NL

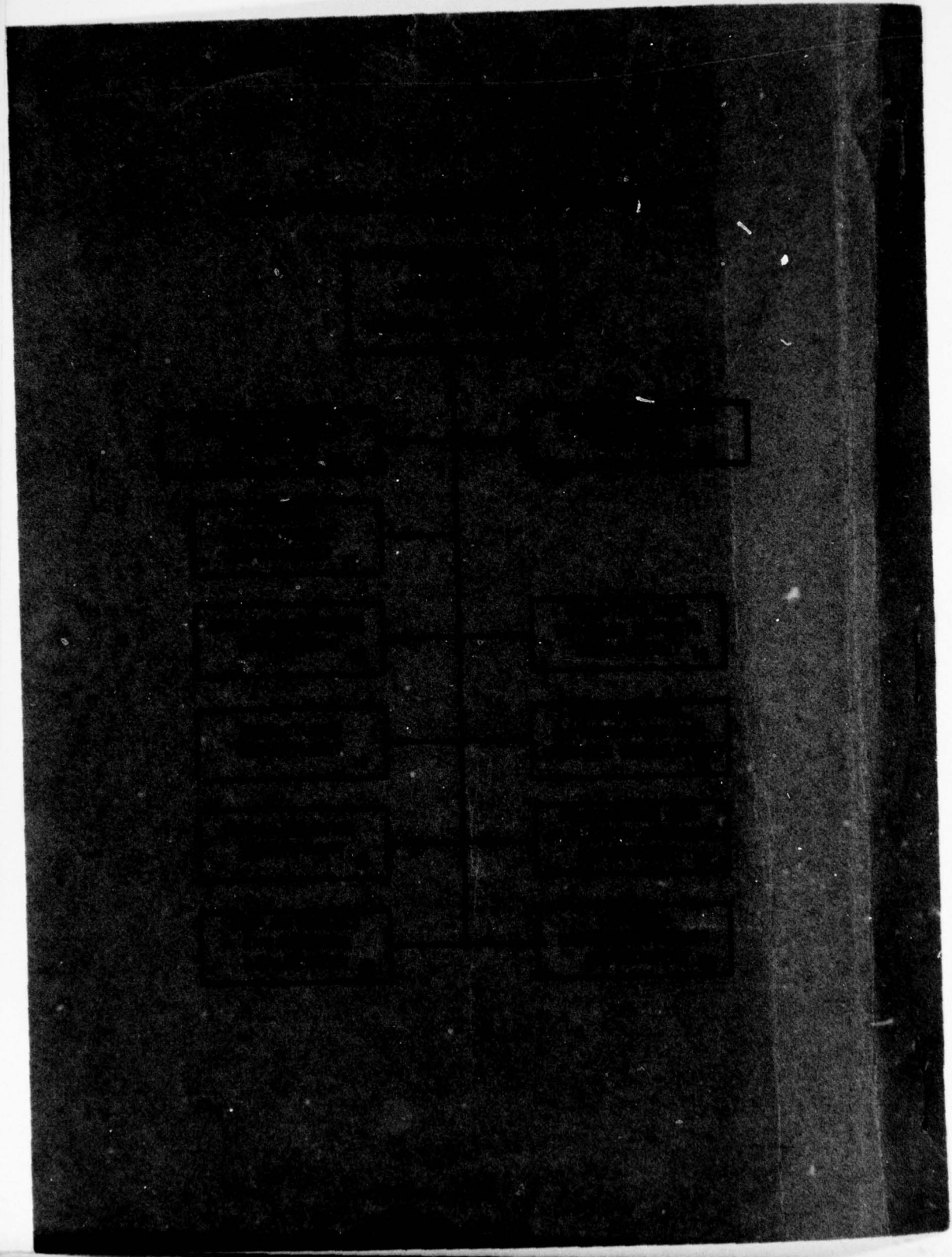
1 of 1
AD
A056 091



END
DATE
FILMED
8-78
DDC

AD A 056091

DIN



UNCLASSIFIED

SECURITY CLASSIFICATION OF THIS PAGE (When Data Entered)

REPORT DOCUMENTATION PAGE		READ INSTRUCTIONS BEFORE COMPLETING FORM
1. REPORT NUMBER DINSRDC-78/054	2. GOVT ACCESSION NO.	3. RECIPIENT'S CATALOG NUMBER
4. TITLE (and Subtitle) ELASTIC-PLASTIC FRACTURE TOUGHNESS (J_{Ic}) OF HIGH-STRENGTH STEELS AND TITANIUM ALLOYS	5. TYPE OF REPORT & PERIOD COVERED Research & Development	
	6. PERFORMING ORG. REPORT NUMBER	
7. AUTHOR(s) John P. Gudas and James A. Joyce	8. CONTRACT OR GRANT NUMBER(s)	
9. PERFORMING ORGANIZATION NAME AND ADDRESS David W. Taylor Naval Ship R&D Center Bethesda, Maryland 20084	10. PROGRAM ELEMENT, PROJECT, TASK AREA & WORK UNIT NUMBERS Work Unit 1-2803-168	
11. CONTROLLING OFFICE NAME AND ADDRESS Naval Sea Systems Command (SEA 035) Washington, D. C. 20062	12. REPORT DATE June 1978	
	13. NUMBER OF PAGES 36	
14. MONITORING AGENCY NAME & ADDRESS (if different from Controlling Office)	18. SECURITY CLASS. (of this report) UNCLASSIFIED	
	15. DECLASSIFICATION/DOWNGRADING SCHEDULE	
16. DISTRIBUTION STATEMENT (of this Report) APPROVED FOR PUBLIC RELEASE: DISTRIBUTION UNLIMITED		
17. DISTRIBUTION STATEMENT (of the abstract entered in Block 20, if different from Report)		
18. SUPPLEMENTARY NOTES		
19. KEY WORDS (Continue on reverse side if necessary and identify by block number) Fracture Toughness J_{Ic} High-Strength Steels J-Integral Elastic-Plastic Test Methods Linear Elastic Titanium Alloys		
20. ABSTRACT (Continue on reverse side if necessary and identify by block number) The elastic-plastic fracture toughness parameter J_{Ic} has been determined for HY 80, HY 130, 10 Ni steel, 17-4PH steel, and titanium alloys Ti-6Al-2Cb-1Ta-0.8Mo, Ti-7Al-2Cb-1Ta, and Ti-6Al-4V. Tests were carried out at room temperature by use of a multiple-specimen test method and a newly developed single-specimen computer interactive test procedure. J_{Ic} is shown to (Continued on reverse side)		

D D C
RECEIVED
JUL 11 1978
RECEIVED

DD FORM 1 JAN 73 1473

EDITION OF 1 NOV 68 IS OBSOLETE
S/N 0102-LF-014-6601

UNCLASSIFIED
SECURITY CLASSIFICATION OF THIS PAGE (When Data Entered)
78 08 11 054

UNCLASSIFIED

SECURITY CLASSIFICATION OF THIS PAGE (When Data Entered)

(Block 20 continue)

be an effective parameter in describing fracture toughness on the basis of both crack initiation and crack-growth resistance. The computer interactive test procedure is shown to produce equivalent results when compared with the multiple-specimen test method and possesses distinct advantages over that method.

ACCESSION No.	
RTM	White Section <input checked="" type="checkbox"/>
RDC	Buff Section <input type="checkbox"/>
UNANNOUNCED	<input type="checkbox"/>
JUSTIFICATION	
BY	
DISTRIBUTION/AVAILABILITY CODES	
REF ID	AVAIL. AND/OR SPECIAL
<input checked="" type="checkbox"/>	<input type="checkbox"/>

UNCLASSIFIED

SECURITY CLASSIFICATION OF THIS PAGE (When Data Entered)

TABLE OF CONTENTS

	Page
LIST OF FIGURES	iii
LIST OF TABLES	iv
LIST OF ABBREVIATIONS	v
ABSTRACT	1
ADMINISTRATIVE INFORMATION	1
INTRODUCTION	1
BACKGROUND	2
LINEAR ELASTIC FRACTURE MECHANICS	2
ELASTIC-PLASTIC FRACTURE MECHANICS	5
SUMMARY OF PUBLISHED J_{Ic} DATA	9
J_{Ic} TESTING	12
MATERIALS	12
TEST PROCEDURES	13
RESULTS AND DISCUSSION	15
CONCLUSIONS	18
ACKNOWLEDGMENTS	18
REFERENCES	27

LIST OF FIGURES

1 - Crack Tip and Equivalent Crack Tip Coordinates	19
2 - Coordinates of J-Integral Contour	19
3 - Crack Tip Deformation Zones	20
4 - 1TCT J_{Ic} Test Specimen (Inches)	21
5 - Computer Interactive J_{Ic} Test Apparatus	21
6 - J_I Versus Crack Extension for HY 80	22

	Page
7 - J_I Versus Crack Extension for HY 130 Steel	22
8 - J_I Versus Crack Extension for 10 Ni Steel	23
9 - J_I Versus Crack Extension for 17-4PH Steel	23
10 - J_I Versus Crack Extension for Ti-6Al-2Cb-1Ta-0.8Mo	24
11 - J_I Versus Crack Extension for Ti-7Al-2Cb-1Ta	24
12 - J_I Versus Crack Extension for Ti-6Al-4V	25
13 - Typical Load Displacement Curve for Single-Specimen Tests (HY 130)	25
14 - J_I Versus Crack Extension from Multiple-Specimen Tests of High-Strength Steels	26
15 - J_I Versus Crack Extension from Multiple-Specimen Tests of Titanium Alloys	26

LIST OF TABLES

1 - Summary of Published J_{IC} Test Data	11
2 - Chemical Composition of Test Alloys	12
3 - Tensile Mechanical Properties of Test Alloys (Transverse Orientation)	13
4 - Summary of J_{IC} Test Results	16

LIST OF ABBREVIATIONS

A/C	Air cool
ASME	American Society of Mechanical Engineers
C	Celsius
cm	Centimeter
dia	Diameter
F	Fahrenheit
hr	Hour
HRR	Hutchinson, Rice and Rosengren
in.	Inch
in-lb/in ²	Inch-pound per square inch
kPa·m	Kilopascal meter
ksi	Thousand pounds per square inch
LEFM	Linear elastic fracture mechanics
mm	Millimeter
mm/min	Millimeter per minute
MPa	Megapascal
MPa·m	Megapascal meter
RA	Reduction in Area
RAM	Read and address memory
ROM	Read only memory
UTS	Ultimate tensile strength
W/Q	Water quench
YS	Yield strength

ABSTRACT

The elastic-plastic fracture toughness parameter J_{Ic} has been determined for HY 80, HY 130, 10 Ni steel, 17-4PH steel, and titanium alloys Ti-6Al-2Cb-1Ta-0.8Mo, Ti-7Al-2Cb-1Ta, and Ti-6Al-4V. Tests were carried out at room temperature by use of a multiple-specimen test method and a newly developed single-specimen computer interactive test procedure. J_I is shown to be an effective parameter in describing fracture toughness on the basis of both crack initiation and crack-growth resistance. The computer interactive test procedure is shown to produce equivalent results when compared with the multiple-specimen test method and possesses distinct advantages over that method.

ADMINISTRATIVE INFORMATION

This study was sponsored by the Naval Sea Systems Command (SEA 03522) and was performed under the Surface Ship Block, Work Unit 1-2803-168. The program manager is Dr. H. H. Vanderfeldt, Naval Sea Systems Command (SEA 03522), and the block principle is Mr. R. J. Wolfe, David W. Taylor Naval Ship Research and Development Center (Code 28).

INTRODUCTION

The use of linear elastic fracture mechanics for the prediction of fracture of flawed structures has been shown to be a useful engineering tool for design and material selection. The development of a standard test method for plane strain fracture toughness indicates that the concepts of LEFM* have been reconciled with empirical results to allow for the reliable measurement of a material property. The use of LEFM is limited, however, to cases of cracked bodies with small-scale yielding. To overcome this, increasing effort has been directed to the formulation of a fracture criterion which would be applicable

*The definitions of abbreviations appear on page v.

for cases of both small- and large-scale plasticity. The path independent J -integral developed in 1968 has emerged as the most promising elastic-plastic fracture concept.

The purpose of this investigation was to evaluate the elastic-plastic fracture toughness parameter, J_{IC} , of several Navy structural alloys. Further, methods for determining J_{IC} were refined. The organization of this report includes an initial review of the concepts of LEFM. The J -integral will then be introduced in a discussion of elastic-plastic fracture mechanics. A review of the J_{IC} data base for structural alloys will be presented. Finally, test results for seven Navy alloys will be developed and test procedures will be detailed.

BACKGROUND

LINEAR ELASTIC FRACTURE MECHANICS

Classical characterization of the mechanical properties of engineering materials has involved the use of parameters from a simple tensile test (yield stress, ultimate tensile strength, elongation, and reduction of area) as the basic properties controlling strength failures of load-bearing structures. Designers have used the material yield strength as the principal design parameter attempting to keep stresses throughout the structure at or below a chosen fraction of the yield stress of the material being used. Considerable ductility is required of engineering materials to blunt local excursions of stress above yield stress such as those seen at fillets or rivet holes.

As materials with increased yield strengths were developed and as stresses were increased, catastrophic failures of an apparently brittle nature were found to occur well before general yielding conditions were present.^{1-3*} Careful examination of

*A complete listing of references is given on page 27.

failures showed generally that rapid crack extension occurred from a preexisting flaw or defect (often a weld flaw or fatigue crack emanating from a region of high local stress). In such cases, the distribution of tensile load across a region containing a preexisting flaw resulted in elevated tensile stress adjacent to the crack tip. In cases where catastrophic rapid crack extension occurred, the elevated tensile stress at the crack tip caused the materials fracture toughness or resistance to crack extension to be exceeded and failure resulted.

The first step in characterizing the resistance of materials to crack extension is to establish the nature of the stress elevation at a crack tip subjected to a tensile load. The stresses and strains near a planar, two-dimensional crack in a large elastic body can be expressed by the following equation:^{4,5}

$$\begin{aligned}\sigma_{ij} &= \frac{K_I}{\sqrt{2\pi r}} S_{ij}(\theta) \\ \epsilon_{ij} &= \frac{K_I}{\sqrt{2\pi r}} E_{ij}(\theta)\end{aligned}\quad (1)$$

where $S_{ij}(\theta)$ and $E_{ij}(\theta)$ are functions of θ as given by Williams⁵ which are on the order of unity, and the origin of coordinates is taken at the equivalent crack tip as shown in Figure 1. The $1/\sqrt{r}$ terms establish the order of the singularity but are independent of the type of crack present, the details of the loading applied, and other geometric details of the cracked body. K_I in these expressions depends on the specific crack and body geometry and the specific loading applied to the body. The K_I term, therefore, sets the stress and strain intensity corresponding to the particular crack geometry and configuration. This term is called the stress intensity factor. Stress intensity factor relationships can be obtained through analytical and experimental techniques⁶⁻⁸ and are tabulated in handbooks by Tada, Paris, Irwin,⁹ and Sih¹⁰ for many crack configuration of interest.

The elastic stresses and strains defined in Equation (1) approach infinity near the crack tip. This is not physically realizable since the material near the tip yields plastically. Analytical estimates given the size of the plastic zone near a crack tip as follows:⁹

$$r_y = \frac{1}{6\pi} \left(\frac{K_I}{\sigma_{ys}} \right)^2 \text{ for plane strain} \quad (2)$$

$$r_y = \frac{1}{2\pi} \left(\frac{K_I}{\sigma_{ys}} \right)^2 \text{ for plane stress} \quad (3)$$

where $2r_y$ is the distance from the crack tip to the furthest extent of the plastic zone, and σ_{ys} is the 0.2 percent offset tensile yield stress. It is a precept of LEFM that as long as the plastic zone is small compared to the distance from the crack tip to the boundary of the specimen or structural component, the elastic singularity "dominates" and fracture initiates (for Mode I opening) when K_I reaches a materials constant, K_{Ic} , regardless of the details of the fracture mechanism within the plastic zone. Recommended practice¹¹ for K_{Ic} determination requires:

$$a, B > 2.5 \left(\frac{K_{Ic}}{\sigma_{ys}} \right)^2 \quad (4)$$

$$W > 5.0 \left(\frac{K_{Ic}}{\sigma_{ys}} \right)^2 \quad (5)$$

where a is the crack length; B is the specimen thickness; and W is the specimen width. By comparison with Equations (2) and (3), this in effect requires the principal specimen dimensions to be on the order of 50 times the size of the plastic zone.

Application of LEFM in design or materials selection involves knowledge of the plane strain fracture toughness property, K_{Ic} , the geometry of cracks present or likely to be

present, and an assessment of the loads likely seen by the component. Utilizing the appropriate stress intensity function, one can assess the maximum allowable crack size for each type of flaw which might exist for each candidate material for a given application.

Combination of LEFM theory with nondestructive test methods has reduced the number of catastrophic failures in structures to which it has been applied. Design and material specifications based on LEFM concepts have been recently adopted by the American Society of Mechanical Engineers as part of the ASME boiler and pressure vessel code,¹² by the American Association of State Highway and Transportation Officials,¹³ and by the United States Air Force¹⁴ among others.

ELASTIC-PLASTIC FRACTURE MECHANICS

Although LEFM is being utilized more commonly, it suffers from limitations of applicability. Fully constrained plasticity requires that LEFM be used for high-strength materials or for very thick sections in a structure. For this reason no valid K_{Ic} data have been obtained for common Navy structural alloys. It is in addressing this limitation, then, that the elastic-plastic fracture toughness parameter J_{Ic} has come to bear.

In 1968, Hutchinson¹⁵ and Rice and Rosengren¹⁶ developed a singularity solution for stresses and strains near a planar, two-dimensional crack in a power hardening elastic-plastic material. This solution can be written in a form similar to that of the elastic solutions (Equation (1)):

$$\frac{\sigma_{ij}(r, \theta)}{\sigma_1} = \left(\frac{J_{Ic}}{\sigma_1 I_N r} \right)^{\frac{N}{N+1}} S_{ij}^*(\theta)$$

$$\epsilon_{ij}(r, \theta) = \left(\frac{J_{Ic}}{\sigma_1 I_N r} \right)^{\frac{1}{N+1}} E_{ij}^*(\theta) \quad (6)$$

where $\bar{\sigma}_1$ = equivalent stress at unit strain
 N = equivalent stress at unit strain
 I_N = function of N given approximately by Shih¹⁷
 $= 10.3 \sqrt{0.13 + N} - 4.8N$
 S_{ij}^*, E_{ij}^* = functions of θ given by Hutchinson¹⁵ which are on the order of unity

In this expression, the following power law hardening stress strain relationship in the nonlinear region is assumed to apply:

$$\bar{\sigma} = \bar{\sigma}_1 (\bar{\epsilon}P)^N \quad (7)$$

This is an asymptotic solution to a nonlinear elastic or deformation plasticity model. Nonetheless, this idealized material has many properties similar to strain hardening elastic-plastic materials of engineering importance.

In the special case of $N=1$, an elastic material is modelled and the J_I singularity reduces to the elastic singularity of Equation (1) (for plane strain), with:

$$J_I = \frac{1-\nu^2}{E} K_{Ic}^2 \quad (8)$$

where E is the elastic modulus, and ν is the Poisson's ratio. Thus, the LFM singularity given by Equation (1) is in fact a special case of the more general Hutchinson, Rice-Rosengren singularity of Equation (6). This suggests that the J_I parameter is the more general and more widely applicable fracture parameter than the LFM parameter K_I .

To evaluate J_I as a function of the specific crack geometries and applied loadings of interest requires using the definition of J_I as a path independent integral given by Rice.¹⁸

$$J_I = \int_{\Gamma} w dy - T_i \frac{\partial u_i}{\partial x} ds \quad (9)$$

where Γ = any contour surrounding the crack tip

$$W = \text{strain energy density} = \int_0^\epsilon \sigma_{ij} d\epsilon_{ij}$$

T_i = traction vector along Γ such that $T_i = \sigma_{ij} n_j$

u_i = displacement vector in the direction of T_i

ds = an element of arc length along Γ

The coordinates for this definition are described in Figure 2. Theoretically, Equation (9) can be used with finite element or other numerical methods to develop empirical equations giving J_I as a function of applied load and crack geometry for structural configurations. In practice, this has not yet been done due to the high costs of deriving the many solutions required. However, Bucci, *et al.*,¹⁹ have shown that for a rigid plastic material, J_I could be evaluated from the following expression:

$$J_I = - \frac{\delta}{B} \left(\frac{\partial P_L}{\partial (\alpha a)} \right) \quad (10)$$

where δ = crack tip opening displacement

B = specimen thickness

P_L = plastic limit load

a = crack length

$\alpha = 1$ for configurations with one crack tip

$\alpha = 2$ for configuration with two crack tips

For example, the solution for the compact tension specimen can be developed by utilizing the limit load expression of Merkle-Corten.²⁰ This yields the following expression after simplification:

$$J_I = 1.26 \sigma_{ys} \left[1 - \frac{\sqrt{2} a}{\sqrt{W^2 + a^2}} \right] \delta \quad (11)$$

where σ_{ys} is the yield stress, W is specimen width, and a is specimen crack length. Other results similarly obtained by Bucci, *et al.*,¹⁹ and Begley, *et al.*,²¹ have shown that J_I depends linearly on a displacement or nominal strain variable.

In review, what has been suggested by various authors and detailed above is that fracture mechanics can be extended into the elastic-plastic regime by using the HRR singularity solution for stress and strain near a sharp crack in a nonlinear elastic solid. The fracture parameter called J_I has been shown to be analogous to K_I and in fact contains the linear elastic solution as a special case. From a physical standpoint, Begley and Landes²² have suggested that when J_I reaches a critical value for the material (J_{Ic}), elastic-plastic crack extension occurs. Again, this is a close analog to the linear elastic case where K_{Ic} is measured at a maximum of 2 percent crack extension under monotonic loading.¹¹

Just as in the case of LEFM, the applicability of the J_I parameter is limited. In the first place, J_I is applicable as a fracture criterion only when the HRR singularity of Equation (6) prescribes the stress and strain conditions at the crack tip. Very close to the crack tip (as depicted in Figure 3) a fracture process zone containing large strains, decohesion zones, voids, and other noncontinuum fracture processes exist. These processes are poorly understood, but because the J_I annular region completely surrounds this zone, the J_I singularity dominates. If this fracture process zone was to grow large compared to the dimensions of the body, J_I would not be an applicable fracture parameter. Long before this would happen though, J_I would fail as a fracture parameter. If the plastic zone extends across the entire specimen and the material strain hardening is low, a transition will take place between the HRR singularity to stress and strain fields defined by rigid plastic nonhardening slip line field theory. In this case, no single fracture parameter would suffice.

Joyce and McClintock²³ investigated two geometries and found the following relationship limits the distance from the crack tip to the nearest boundary:

$$b > 2 \left(\frac{\bar{\sigma}_1}{\sigma_{ys}} \right)^{\frac{1}{N}} \frac{J_{Ic}}{I_N \sigma_{ys}} \quad (12)$$

where b is the distance from the crack tip to the nearest boundary and $\bar{\sigma}_1$, N , σ_{ys} , and I_N are as defined previously. Similarly, Paris²⁴ has suggested that the specimen thickness satisfy the following relation for a J_{Ic} test to be valid:

$$B > (25 \text{ to } 40) \frac{J_{Ic}}{\sigma_{ys}} \quad (13)$$

Very little data is available to validate either relationship.

Landes and Begley²² and Paris²⁵ have pointed out that any crack extension implies material unloading in the vicinity of the crack front which violates assumptions of the J-integral analysis which produced Equation (6). J_{Ic} is defined for the first increment of crack extension, but it is obtained by extrapolating back from a $J-\Delta a$ resistance curve for which crack extension is the abscissa. Logsdon²⁶ has compared K_{Ic} values obtained from J_I with ASTM-E399 K_{Ic} values and has shown that close agreement is obtained. Until a test method for J_{Ic} determination is developed which does not require extrapolation from a $J-\Delta a$ resistance curve, the role of unloading due to crack extension is open to question.

SUMMARY OF PUBLISHED J_{Ic} DATA

Because the development of an elastic-plastic fracture criterion is of great importance to the pressure vessel and power generation industries, much of the published J-integral data reflects interest in materials commonly used in these industries. In their initial paper evaluating the J-integral as a fracture criterion, Begley and Landes²² reported test results for ASTM A533B Class 2 pressure vessel steel and an

intermediate strength Ni-Cr-Mo-V rotor steel. Table 1 presents the mechanical properties and J_{IC} values for these materials and others which will be discussed throughout this section. Three specimen types including 20 mm (0.79 inch) bend bars, 25 mm (1 inch) (1TCT), and 50 mm (2 inch) (2TCT) thick compact tension specimens of A533B steel were tested. The A533B steel was tested at room temperature while the rotor steel was tested at 200 F (93 C), the start of upper shelf K_{IC} behavior. The values of J_{IC} reported were determined from the maximum load, a practice which was subsequently found to overestimate J_{IC} . Experiments with the same Ni-Cr-Mo-V rotor steel using several specimen types were then carried out by Landes and Begley²⁷ to evaluate the effects of different plastic slip-line fields. Again, J_{IC} was evaluated at maximum load and the range of results is included in Table 1. ASTM A216 WCC grade cast steel of relatively low strength and high toughness was then evaluated by Landes and Begley²⁸ to establish a J_{IC} testing procedure and evaluate the equivalence of J_{IC} and K_{IC} values over a range of temperatures. In this effort, curves of J_I versus crack extension (Δa) were constructed for multiple specimen tests to allow examination of alternate J_{IC} measurement points. The test results for six different specimen geometries taken at the intersection of the best fit line of the crack extension points to the crack opening stretch line ($J = 2\sigma_{flow}\Delta a$) resulted in a narrow range of J_{IC} values shown in Table 1.

Logsdon²⁶ provided a comprehensive evaluation of the elastic-plastic fracture of rotor forging steels. The steels investigated included ASTM A471 Ni-Cr-Mo-V, ASTM A469 Ni-Mo-V, ASTM A470 Cr-Mo-V, AISI 403 modified 12-Cr rotor forging steel, and ASTM A217 2 1/4 Cr-1 Mo cast steel. This work is important because 1TCT specimens were removed from heats of these steels for which corresponding K_{IC} values had been obtained. The Landes-Begley resistance curve technique was employed and tests were carried out over a temperature range from 10-24 C (18-43 F)

above the maximum temperature where valid K_{IC} values were generated with 1TCT specimens to the temperature where 0 percent brittle fracture first occurred in Charpy V-notch test results. Logsdon showed that K_{IC} evaluated from J_{IC} results corresponded closely with valid K_{IC} results obtained specimens as large as 8TCT.

TABLE 1 - SUMMARY OF PUBLISHED
 J_{IC} TEST DATA

Material	Refer- ence	YS MPa	UTS MPa	Elonga- tion %	RA %	J_{IC} Test Temperature C	J_{IC} KPa·m	Comments
ASTM A533B CL2	22	483				24	165-180	HSST material
Ni-Cr-Mo-V Steel	22	917	1021	16		93	149-173	
Ni-Cr-Mo-V Steel	27	917	1021	16		121	172-187	
A216WCC Cast Steel	28	303	510	16	34	121	289-315	ITCT-4TCT specimens only
Ni-Cr-Mo-V Steel	26	931	1023	16.6	56.7	65 121	105 123	
Ni-Mo-V Steel	26	590	721	21.8	62.5	149	140	
Cr-Mo-V Steel	26	626	784	17.1	46.9	149	81	
AISI 403 MOD 12 Cr	26	682	821	16.8	48.5	200 149	83 70	
2 1/4 Cr-1Mo Cast Steel	26	419	573	17.6	42.8	-46 24	162 140	
Ti-6Al-4V	29	858	923	13.5	39.5	24	33-43	
Al 2024-T 351	30	338	492	21.5	23.5	24	15	B = 2.36 cm
Al 7005-T 6351	30	358	408	12.5	29.0	24	22	Center plate B = 2.24 cm
Ni-Cr-Mo-V Steel	31	770	893	20.6	61.1	149	105	CT specimens only, fatigue precracked
Al 6061-T 651	31	276	324	14	32	24	16	Fatigue pre- cracked
HY 130	32	986	1048	21.0	68	24	215	$J = \frac{2U}{B(W-a)}$

Yoder and Griffis²⁹ evaluated the elastic-plastic fracture toughness of Ti-6Al-4V with 3-point bend bars of two different thicknesses and crack lengths. Again the Landes-Begley resistance curve was employed, and results are shown in Table 1. Subsequently, Griffis and Yoder³⁰ evaluated the J_{IC} of two aluminum alloys, 2024-T351 and 7005-T6351. The results shown in Table 1 are derived from the multiple specimen resistance curve technique using 3-point bend bars.

Begley and Logsdon³¹ evaluated J_{IC} of ASTM A471 Ni-Cr-Mo-V rotor steel and Al 6061 T6. Various specimen geometries and root radii were evaluated, and the results shown in Table 1 cover only tests employing fatigue cracks. This is the first attempt to show empirically that J_{IC} provides a convenient engineering technique to predict fracture behavior of engineering structures containing notch-like defects of finite-root radius.

Most recently, Kamath and Harrison³² evaluated ductile crack extension criteria in HY 130 steel. Both J_I and COD were evaluated, and results of test methods and computational methods are reported. Table 1 includes their J_{IC} test results developed by using single-edge notch cantilever beam specimens and employing the multiple-specimen test method.

J_{IC} TESTING

MATERIALS

Seven alloys were evaluated in the test program reported herein. These included HY 80, HY 130, 10 Ni-Co-Cr-Mo and 17-4PH steels, and titanium alloys Ti-6Al-2Cb-1Ta-0.8Mo, Ti-7Al-2Cb-1Ta, and Ti-6Al-4V. The chemical composition and tensile mechanical properties of these materials are presented in Tables 2 and 3, respectively. All materials were supplied in the form of rolled plate.

TABLE 2 - CHEMICAL COMPOSITION OF TEST ALLOYS

Material (Code)	C	Mn	P	Si	Ni	Cr	Mo	V	S	Cb	Ta	Cu	Al	Co	Ti
Steels, Chemical Composition (Weight Percent)															
HY 80 (EPI)	0.158	0.29	0.009	0.31	2.99	1.55	0.44	0.015	0.020			0.18			
HY 130 (FKS)	0.11	0.76	0.005	0.31	5.00	0.42	0.53	0.043	0.004			0.022	0.021	0.02	0.008
10 Ni Steel (E2C)	0.12	0.11	0.007	0.07	10.26	1.99	1.007		0.003					7.75	0.002
17-4PH (ENU)	0.037	0.20	0.023	0.57	4.28	15.99			0.011	0.27	0.01	3.3			
Titanium Alloys, Chemical Composition (Weight Percent)															
Material (Code)	C	N	Fe	Al	Cb	Ta	Mo	O	H	V					
Ti-6Al-2Cb-1Ta-0.8Mo (FBS)	0.02	0.014	0.05	5.8	1.9	0.92	0.80	0.94	0.0052						
Ti-7Al-2Cb-1Ta (FAR)	0.010	0.0057	0.12	6.52	2.22	1.35		0.032	0.0052						
Ti-6Al-4V (FGU)	0.021	0.012	0.197	6.25				0.15	0.0031	3.95					

TABLE 3 - TENSILE MECHANICAL PROPERTIES
OF TEST ALLOYS (TRANSVERSE ORIENTATION)

Alloy (Code)	Heat Treatment	0.2% YS MPA (ksi)	UTS MPa (ksi)	Elong- tion % in 2 in.	Reduction of Area %
HY 80 (EFI)	900 C, 1 hr, W/Q 690 C, 1 hr, W/Q	544 (79)	679 (99)	27	66
HY 130 (FKS)	830 C, 1.5 hr, W/Q 630 C, 1.5 hr, W/Q	937 (136)	978 (142)	21	55
10 Ni Steel (Ezc)	885 C, 1 hr, W/Q 815 C, 1 hr, W/Q 510 C, 5 hr, W/Q	1300 (180)	1452 (211)	19	69
17-4PH (ENU)	1040 C, 1 hr, A/C 590 C, 4 hr, A/C	883 (128)	972 (141)	11	64
Ti-6Al-2Cb- 1Ta-0.8Mo (FBS)	As received Hot rolled	700 (101)	792 (115)	13	23
Ti-7Al-2Cb-1Ta (FAR)	1090 C, 1 hr, A/C	665 (96)	741 (108)	10	23
Ti-6Al-4V (FGU)	-	822 (119)	934 (136)	11	16

TEST PROCEDURES

Modified compact tension specimens were produced from each material according to Figure 4. This specimen allows for clip gage placement on the load line. In all cases, the crack plane was placed in the T-L orientation. All specimens were fatigue precracked as per ASTM E399-74 to a total "notch" depth of 38 mm (1.5 inch), that is $a/W = 0.75$, where a is the crack length and W is the specimen width. All elastic-plastic fracture toughness tests were carried out at room temperature with a displacement controlled test machine. Maximum cross-head speed was 0.25 mm/min. The multiple-specimen test procedure was as suggested by Landes and Begley.²⁸ The specific steps in this test sequence and data analysis are as follows:

1. For each material, at least four individual specimens were loaded to different crack opening displacement values, and corresponding load-displacement plots were produced.

2. Individual specimens were then unloaded, and the cracks were marked by heat tinting. For steels, the heat tinting was accomplished by placing specimens in a furnace at 370 C for

1/2 hour followed by air cooling. Titanium alloys were heated to 760 C for a similar period followed by air cooling. Specimens were then pulled apart at liquid nitrogen temperature to minimize plasticity effects during separation.

3. Crack extension was measured with a travelling stage microscope over nine evenly spaced points, including the center line of each specimen and excluding the points at each side of the specimen.

4. J_I values were calculated from the load point displacement curve for each specimen according to the relation $J_I = 2A/Bb$; where A is the area under the curve to the point of unloading; B is the specimen thickness; and b is the uncracked ligament measured from the end of the crack.

5. For each alloy tested, a plot of J_I versus crack extension (Δa) was constructed. A least squares straight line was fit to all data with Δa greater than $J_I/2\sigma_{flow} + 0.05$ mm where $\sigma_{flow} = (\sigma_{ys} + \sigma_{UTS})/2$. J_{IC} was taken as the intersection of the above line and the crack opening stretch line $J_I = 2\sigma_{flow}\Delta a$.

6. Validity analysis was carried out according to the criterion:

$$B \geq 40 \frac{J_I}{\sigma_{ys}}$$

Single specimen tests utilized a computer interactive test procedure uniquely developed for J_{IC} evaluation. The key requirement for carrying out a single specimen test for J_{IC} is the ability to accurately measure crack length at a series of points along a load-displacement record. In this program, compliance measurements were taken during short unloadings along the load-displacement record to estimate crack length and crack advance. A schematic of the computer interactive test system employed for this purpose is shown in Figure 5. Analog signals from the clip gage and load transducer are digitized and read by the computer approximately once per second. These data

are stored on tape and plotted as a real time load versus COD plot. During the test, several unloadings on the order of 10 percent of the maximum load are carried out. For each unloading the area under the load-displacement curve is computed and a linear regression fit of the slope of the unloading line is used to estimate the present crack length and crack extension from the following compliance expression:

$$\frac{a}{W} = 1.000196 - 4.06319 U_{LL} + 11.242 U_{LL}^2 - 106.043 U_{LL}^3 + 464.355 U_{LL}^4 - 650.677 U_{LL}^5 \quad (14)$$

where

$$U_{LL} = \frac{1}{\left(\frac{BE\delta}{(1-\nu)P} \right)^{1/2} + 1}$$

and δ/P is the specimen load line compliance.¹⁴ A unique J_I versus Δa pair is obtained for each unloading and, in turn, stored on magnetic tape. At the conclusion of test, a plot of J_I versus Δa from the compliance estimate was produced and J_{IC} was estimated by the criteria outlined in the multiple specimen test method. Single-specimen tests were performed with HY 130, 10 Ni steel, 17-4PH steel, as well as titanium alloys Ti-7Al-2Cb-1Ta and Ti-6Al-4V.

RESULTS AND DISCUSSION

Specific J_{IC} values for multiple- and single-specimen tests are reported in Table 4 including a summary of specimen validity calculations and equivalent K_{IC} calculations from Equation (8). The J_I versus crack extension resistance curves for HY 80, HY 130, 10 Ni steel, 17-4PH steel, and titanium alloys Ti-6Al-2Cb-1Ta-0.8Mo, Ti-7Al-2Cb-1Ta, and Ti-6Al-4V are presented in Figures 6-12, respectively. Each of these figures shows the blunting line and least squares linear regression fit of individual data points. The intersection of these two lines defines

the critical J_I for initiation of crack extension. Figure 13 presents a typical load-displacement curve for single-specimen tests (HY 130) showing periodic unloadings to develop crack extension estimates.

TABLE 4 - SUMMARY OF J_{IC} TEST RESULTS

Material	J_{IC} KPa·m (in-lb/in ²)		Specimen Thickness mm (in.)	$40 J_{IC}/\sigma_{ys}$ mm (in.)		Eq K_{Ic} MPa·m ^{1/2} (ksi·in. ^{1/2})	
	Specimen			Specimen		Specimen	
	Multiple	Single		Multiple	Single	Multiple	Single
HY 80 (EFI)	81 (465)	-	25.1 (0.990)	6.0 (0.24)	-	134 (122)	-
HY 130 (FKS)	186 (1060)	208 (1184)	25.1 (0.990)	7.9 (0.31)	8.9 (0.35)	202 (184)	213 (194)
10 Ni Steel (E2C)	118 (673)	138 (788)	25.2 (0.994)	3.6 (0.14)	4.2 (0.17)	161 (146)	174 (158)
17-4PH (ENU)	106 (607)	112 (641)	25.4 (1.000)	4.6 (0.18)	4.8 (0.19)	153 (139)	157 (143)
Ti-6Al-2Cb- 1Ta-0.8Mo (FBS)	108 (614)	-	25.4 (1.000)	6.2 (0.24)	-	117 (108)	-
Ti-7Al-2Cb-1Ta (FAR)	71 (405)	73 (419)	25.8 (1.015)	4.3 (0.17)	4.4 (0.17)	96 (87)	97 (88)
Ti-6Al-4V (FGU)	39 (225)	48 (272)	25.4 (1.001)	1.9 (0.07)	2.3 (0.09)	71 (65)	78 (71)

Figure 14 is a compilation of multiple-specimen data for the four steels tested. The data suggest the dual analysis available with J_{IC} testing. The superior fracture toughness of HY 130 in comparison with 17-4PH of similar yield strength and 10 Ni steel is obvious. The slopes of the $J-\Delta a$ resistance curves decrease monotonically with increasing yield strength. When considering HY 80, the combination of low J_{IC} and high $J-\Delta a$ slope implies that HY 80 is less resistant to crack initiation but is more resistant to crack extension beyond 1 mm than any of the steels tested.

Lacking other valid fracture toughness values for these steels, the data presented in Table 4 provide the best description of their fracture toughness properties. The HY 130 data

presented suggest that 6T (150 mm) compact tension specimen tests would be required to produce valid plane strain K_{IC} results.

The multiple-specimen $J-\Delta a$ data for the three titanium alloys is presented in Figure 15. This figure points up the wide variation in fracture toughness values with similar $J-\Delta a$ resistance curve slopes. The data shows that for this class of alloys, J_{IC} clearly discriminates on the basis of crack initiation. The calculated K_{IC} value for Ti-6Al-4V indicates that this material, possessing an acicular alpha microstructure with evidence of prior beta grain boundaries, is on the lower bound of published valid K_{IC} data for the alloy.³⁴

Analysis of multiple- and single-specimen test data shows that both test methods produce equivalent J_{IC} values. The data in Table 4 shows that the J_{IC} from single-specimen tests runs from 3 to 21 percent higher than J_{IC} from multiple-specimen tests. With the exception of Ti-7Al-2Cb-1Ta, the single specimen method consistently produces higher $J-\Delta a$ resistance curve slopes. This results from the fact that considerable crack front curvature existed with all materials except Ti-7Al-2Cb-1Ta. When cracks tunnel, the compliance-calculated crack length is smaller than the average of nine measured points across the specimen. At this time, there is a question regarding the best method to characterize actual crack extension. Final 9-point average crack length measurements shown on Figures 7, 8, 9, and 11 suggest equivalence between single- and multiple-specimen tests when identical crack length measurements are used.

The single-specimen test method is preferable to the multiple-specimen method for several reasons. The single specimen method produces a J_{IC} and a $J-\Delta a$ resistance curve for each test. When several specimens are available, the multiplicity of J_{IC} values allows for statistical analysis of material variability. The single-specimen method allows for J_{IC} tests to be carried out in various environments and over ranges of temperatures. The large number of data points allows for better

analysis of the slope and shape of the $J-\Delta a$ resistance curve. Lastly, this method is more likely to be applicable in quality assurance testing of Navy structural alloys.

CONCLUSIONS

1. J_{IC} fracture toughness values have been measured for HY 80, HY 130, 10 Ni steel, 17-4PH steel, Ti-6Al-2Cb-1Ta-0.8Mo, Ti-7Al-2Cb-1Ta, and Ti-6Al-4V. These data provide valid characterization of fracture toughness properties in the elastic-plastic regime.

2. J_I is seen as an effective parameter in describing fracture toughness and distinguishes between toughness at crack initiation and resistance to crack extension.

3. In the case of Ti-6Al-4V, J_{IC} was shown to predict valid plane strain fracture toughness values.

4. A computer interactive single-specimen test method has been developed and shown to be equivalent to the multiple-specimen method. The advantages of the single-specimen method include more efficient use of available material, greater detail in test data, multiplicity of J_{IC} values for analysis of material variability, and potential to test over a range of environments and temperatures.

ACKNOWLEDGMENTS

The authors wish to thank Mr. R. J. Stockhausen for assistance in specimen preparation and Mr. J. Keith Donald of DEL Research Corporation for advice in developing single-specimen test procedures.

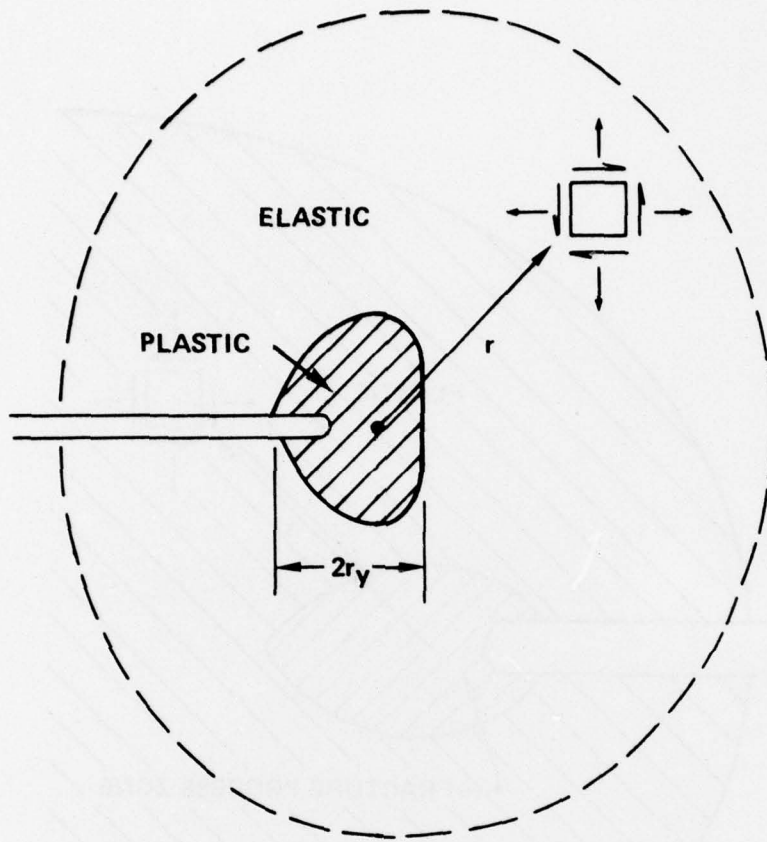


Figure 1 - Crack Tip and Equivalent Crack Tip Coordinates

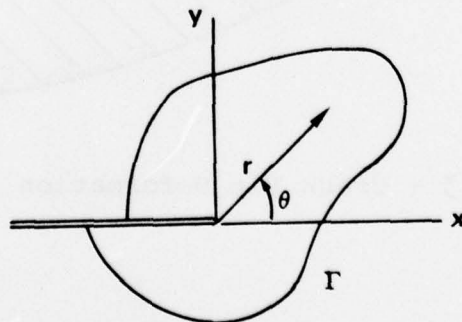


Figure 2 - Coordinates of J-Integral Contour

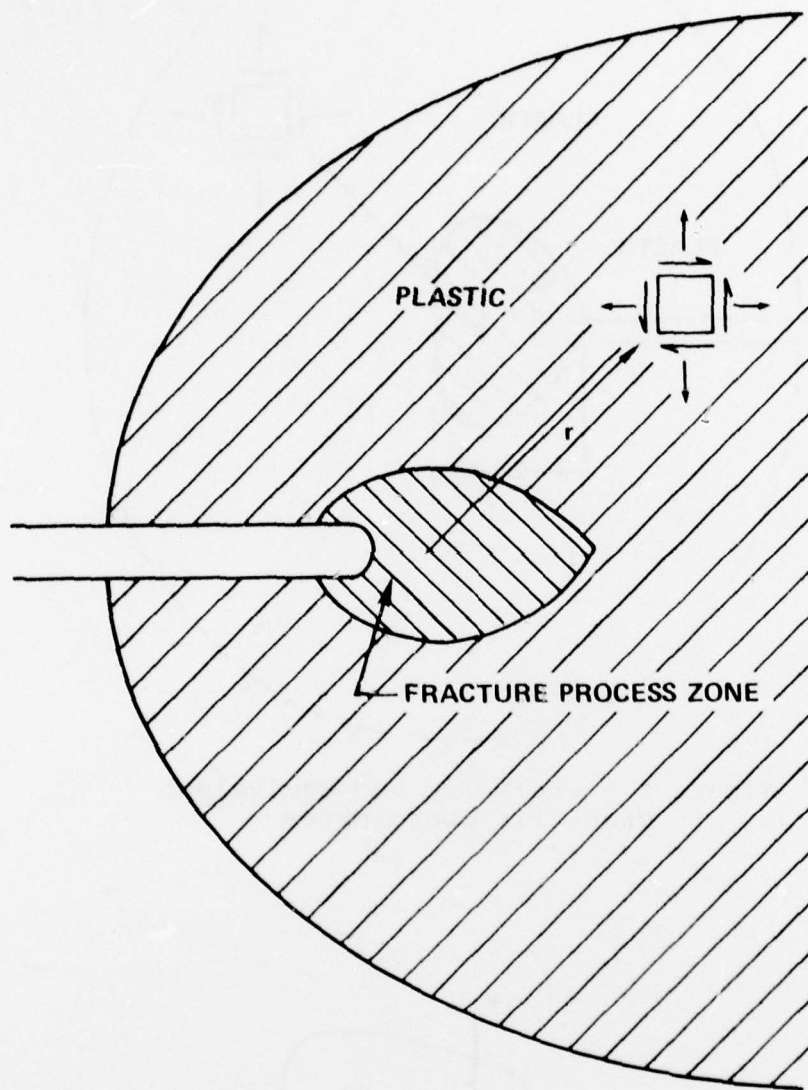


Figure 3 - Crack Tip Deformation Zones

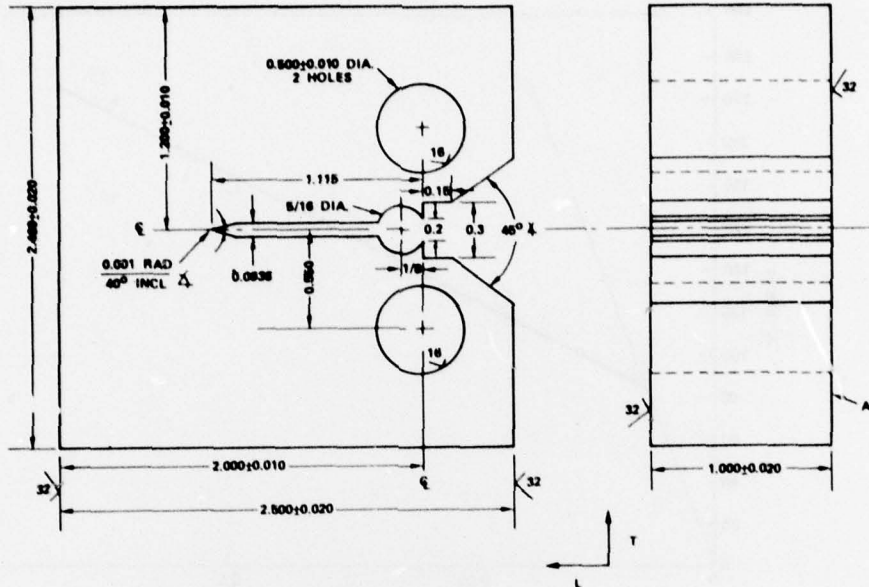


Figure 4 - 1TCT J_{Ic} Test Specimen
(Inches)

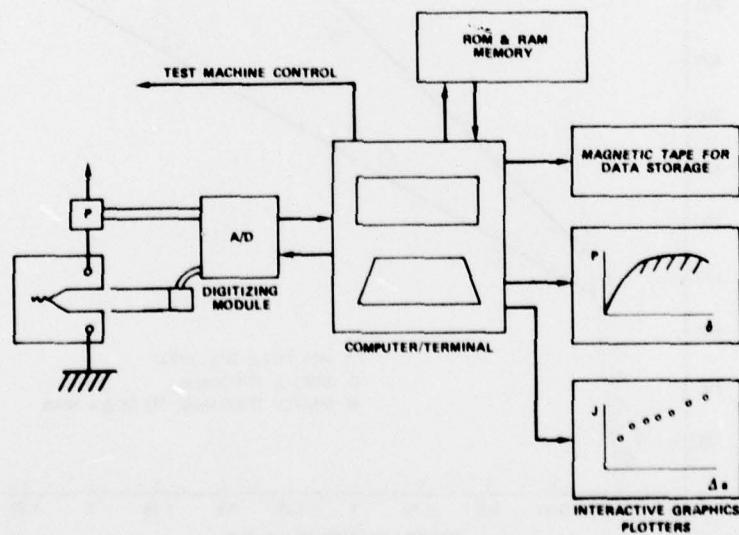


Figure 5 - Computer Interactive
 J_{Ic} Test Apparatus

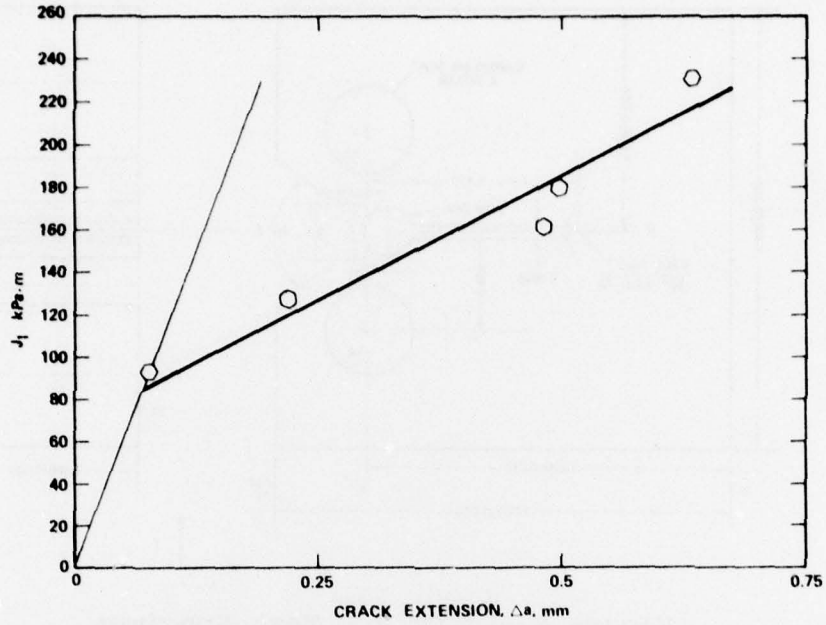


Figure 6 - J_I Versus Crack Extension for HY 80

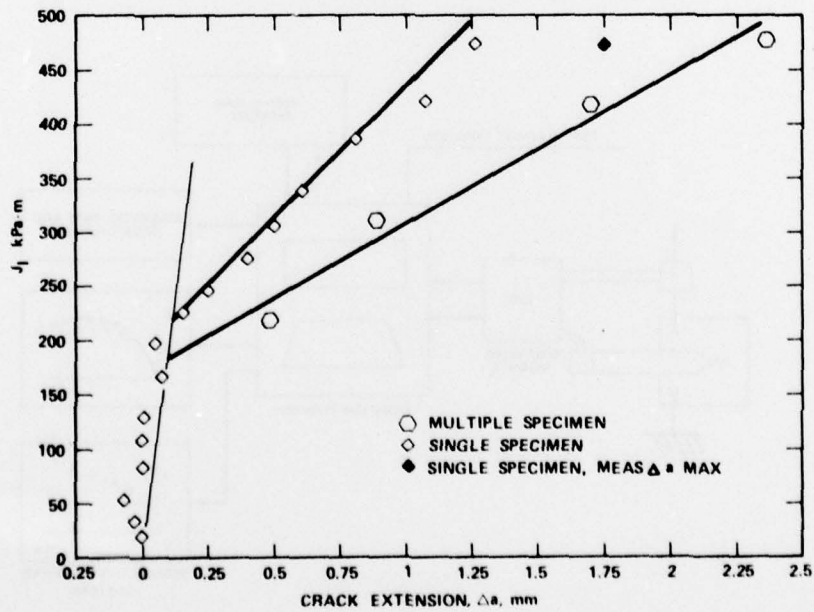


Figure 7 - J_I Versus Crack Extension for HY 130 Steel

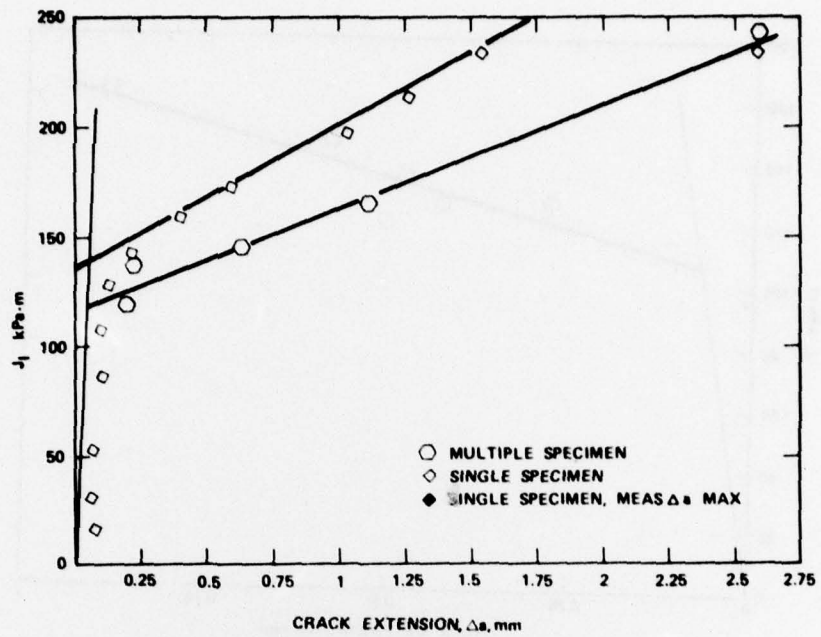


Figure 8 - J_I Versus Crack Extension for 10 Ni Steel

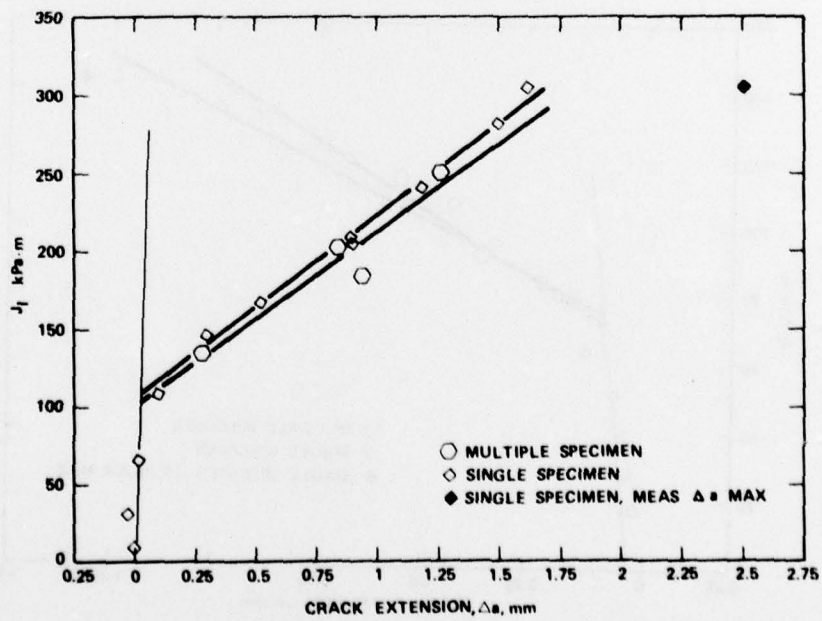


Figure 9 - J_I Versus Crack Extension for 17-4PH Steel

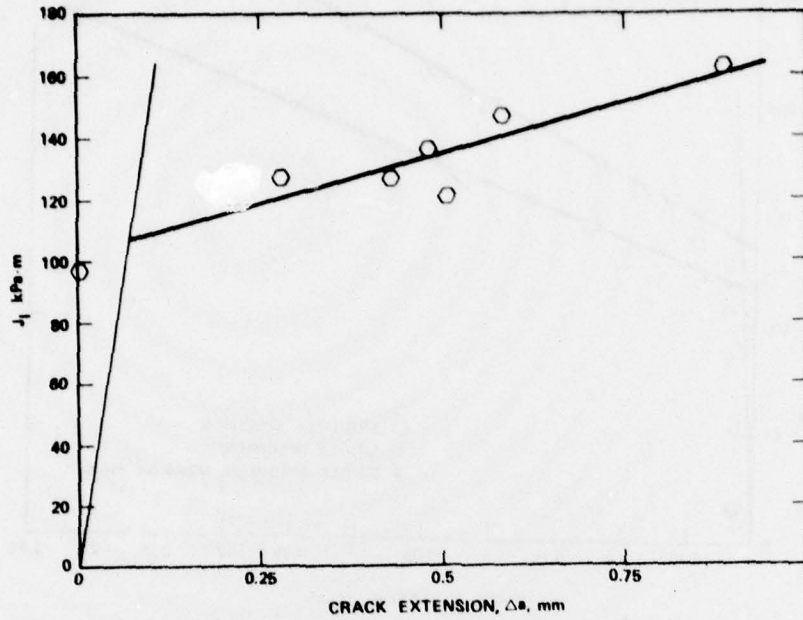


Figure 10 - J_I Versus Crack Extension for Ti-6Al-2Cb-1Ta-0.8Mo

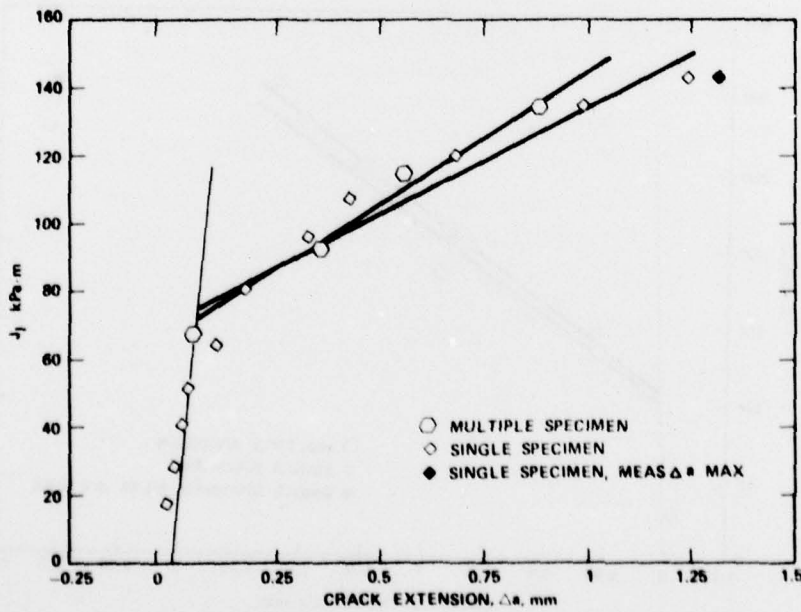


Figure 11 - J_I Versus Crack Extension for Ti-7Al-2Cb-1Ta

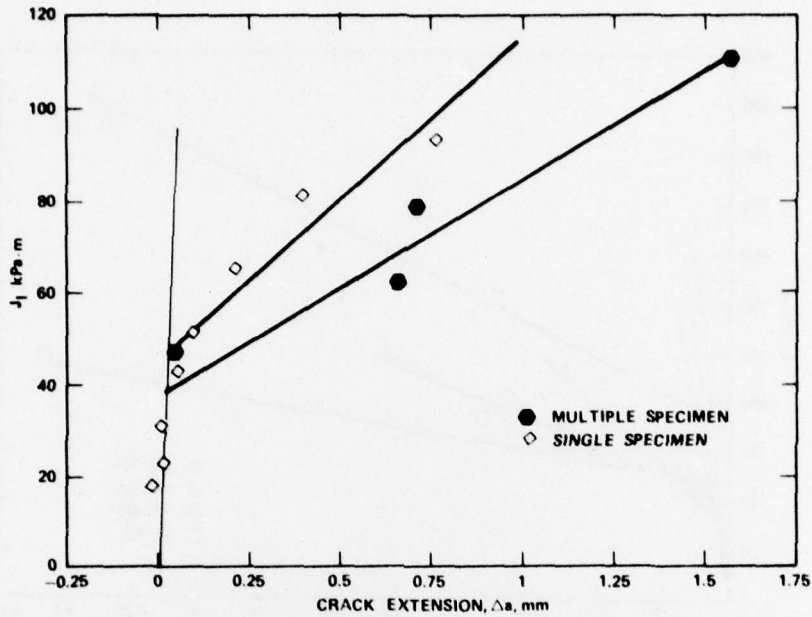


Figure 12 - J_I Versus Crack Extension for Ti-6Al-4v

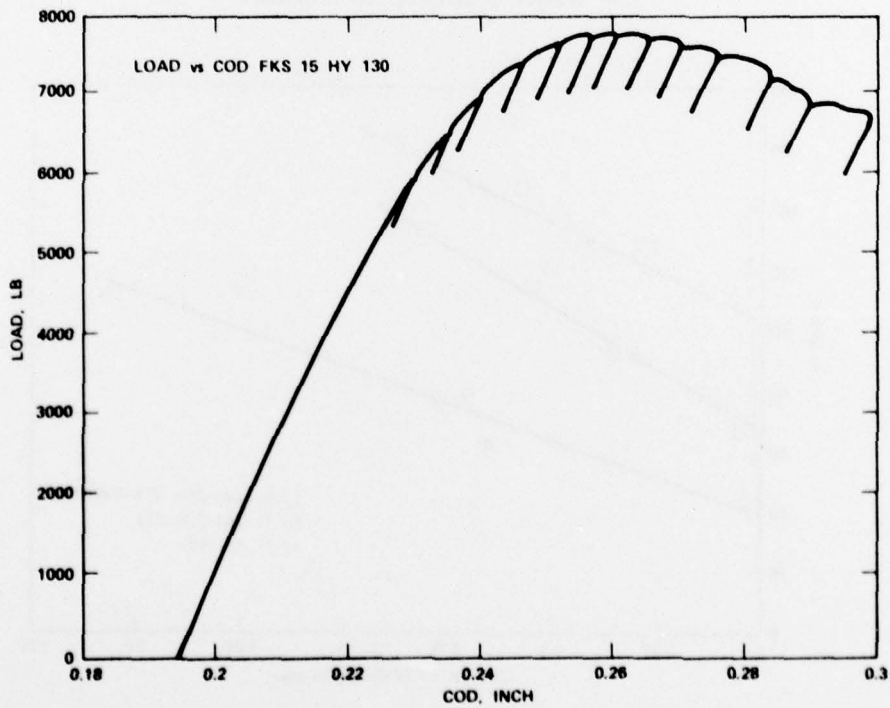


Figure 13 - Typical Load Displacement Curve for Single-Specimen Tests (HY 130)

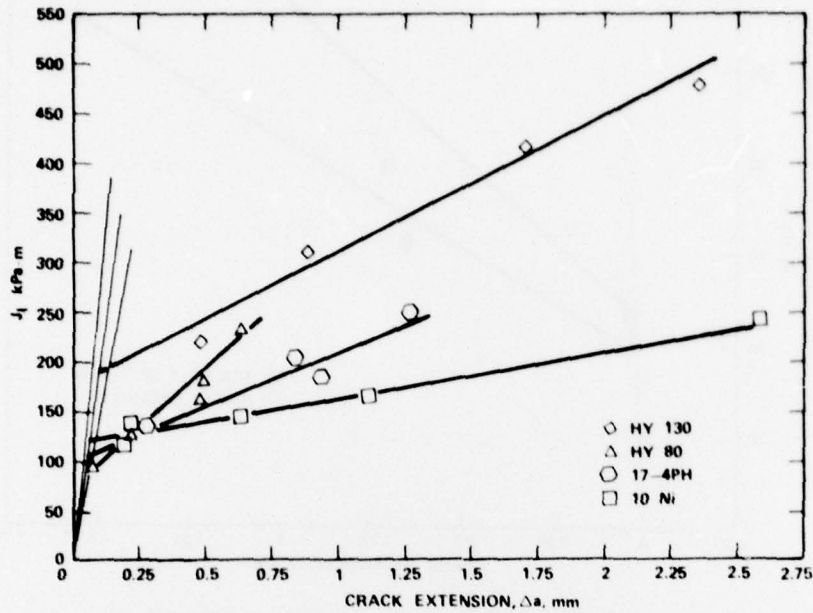


Figure 14 - J_I Versus Crack Extension from Multiple-Specimen Tests of High-Strength Steels

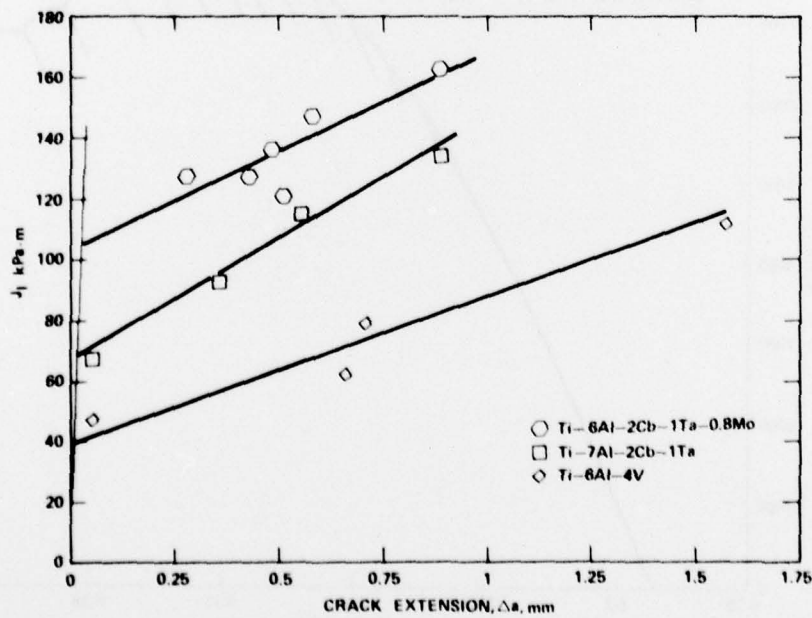


Figure 15 - J_I Versus Crack Extension from Multiple-Specimen Tests of Titanium Alloys

REFERENCES

1. Bishop, T., "Fatigue and the Comet Disaster," Metal Progress, Vol. 67, pp. 77-85 (May 1955).
2. "Collapse of US 35 Highway Bridge, Point Pleasant, West Virginia," National Transportation Safety Board Rept NTSB-HAR-71-1 (19 Dec 1967).
3. Bennet, J. A., and H. Mindlin, "Metallurgical Aspects of the Failure of the Point Pleasant Bridge," Journal of Testing and Evaluation, pp. 152-161 (Mar 1973).
4. Irwin, G. R., "Analysis of Stresses and Strains Near the End of a Crack Traversing a Plate," Journal of Applied Mechanics, Vol. 24, pp. 361-364 (1957).
5. Williams, M. L., "On the Stress Distribution at the Base of a Stationary Crack," Journal of Applied Mechanics, Vol. 24, pp. 109-114 (1957).
6. Srawley, J. E., et al, "Experimental Determination of the Dependence of Crack Extension Force on Crack Length for a Single-Edge Notch Tension Specimen," NASA Tech Rept TN-D-2396 (1964).
7. Sih, G. C., editor, Methods of Analysis and Solutions of Crack Problems, Leyden, Netherlands, Noordhoff Int. (1973).
8. Kobayaski, A. S., Experimental Techniques in Fracture Mechanics, SESA Monograph 1, Ames, Iowa, Iowa State Univ. Press (1973).
9. Tada, H., et al, The Stress Analysis of Crack Handbook, Hellertown, PA, DEL Research Corp. (1973).
10. Sih, G. C., Handbook of Stress Intensity Factors for Researchers and Engineers, Bethlehem, PA, Lehigh Univ. Press, (1973).
11. Standard Method of Test for Plane Strain Fracture Toughness of Metallic Materials, ASTM E 399-74, Annual Book of ASTM Standards, Philadelphia, PA (1975).

12. ASME Boiler and Pressure Vessel Code, Section III, G ASME, New York (1972).
13. American Association of State Highway and Transportation Officials, Materials Specifications, Wash., D.C. (1974).
14. MIL-STD 1530, Aircraft Structural Integrity Program, Airplane Requirements, USAF (1972).
15. Hutchinson, J. W., "Singular Behavior at the End of a Tensile Crack in a Hardening Material," Journal of Mechanics and Physics of Solids, Vol. 16, pp. 13-31 (1968).
16. Rice, J. R., and G. F. Rosengren, "Plane Strain Deformation Near Crack Tip in a Power Law Hardening Material," Journal of Mechanics and Physics of Solids, Vol. 16, pp. 1-12 (1968).
17. Shih, C. F., "Small Scale Yielding Analysis of Mixed Mode Plane-Strain Crack Problems," ASTM STP 560, Philadelphia, PA, pp. 187-210 (1973).
18. Rice, J. R., "A Path Independent Integral and the Approximate Analysis of Strain Concentration by Cracks and Notches," Journal of Applied Mechanics, Vol. 35, pp. 379-386 (1968).
19. Bucci, R. J., et al, "J Integral Estimation Procedures," ASTM STP 514, pp. 40-69 (1972).
20. Merkle, J. G., and H. T. Corten, "A J-Integral Analysis for the Compact Specimen, Considering Axial Force as Well as Bending Effects," Transactions of the ASME, pp. 286-292 (Nov 1974).
21. Begley, J. A., et al, "An Estimation Model for the Application of the J-Integral," ASTM STP 560, pp. 155-169 (1973).
22. Begley, J. A., and J. D. Landes, "The J-Integral as a Fracture Criterion," ASTM STP 514, Philadelphia, PA, pp. 1-20 (1972).

23. Joyce, J. A., and F. A. McClintock, "Predicting Ductile Fracture Interaction in Large Parts," Strength and Structure of Solid Materials, Leyden, Netherlands, Noordhoff Int., pp. 157-181 (1976).
24. Paris, P. C., Written Discussion to: "The J-Integral as a Fracture Criterion," by J. A. Begley and J. D. Landes, ASTM STP 514, Philadelphia, PA., pp. 21-22 (1972).
25. Paris, P. C., "Fracture Mechanics in the Elastic-Plastic Regime," ASTM STP 631, Philadelphia, PA., pp. 3-27 (1977).
26. Logsdon, W. A., and J. A. Begley, "Upper Shelf Temperature Dependence of Fracture Toughness for Four Intermediate Strength Pearlitic Steels," Engineering Fracture Mechanics, Vol. 6, pp. 461-470 (1977).
27. Landes, J. D., and J. A. Begley, "The Effect of Specimen Geometry on J_{IC} ," ASTM STP 514, Philadelphia, PA., pp. 24-39 (1972).
28. Landes, J. D., and J. A. Begley, "Test Results from J-Integral Studies: An Attempt to Establish a J_{IC} Testing Procedure," ASTM STP 560, Philadelphia, PA., pp. 170-186 (1973).
29. Yoder, G. R., and C. A. Griffis, "J-Integral and the Initiation of Crack Extension in a Titanium Alloy," NRL Rept 7662 (Feb 1974).
30. Griffis, C. A., and G. R. Yoder, "Initial Crack Extension in Two Intermediate Strength Aluminum Alloys," Journal of Engineering Materials and Technology, Vol. 98 (Apr 1976).
31. Begley, J. A., and W. A. Logsdon, "A Ductile Rupture Blunt Notch Fracture Criterion," ASTM STP 631, Philadelphia, PA., pp. 112-120 (1977).
32. Kamath, B. S., and J. D. Harrison, "Ductile Crack Extension in API 52 X65 and HY 130 Steels," The Welding Institute, Cambridge, UK, 36/1977/E (Apr 1977).

33. Saxena, A., and S. J. Hudak, Jr., "Review and Extension of Compliance Information for Common Crack Growth Specimens," Westinghouse Scientific Paper 77-9E7-AFCGR-P1 (May 1977).

34. Campbell, J. E., et al, Damage Tolerant Design Handbook, Columbus, Ohio, MCIC, Battelle Columbus Laboratories (1972).

INITIAL DISTRIBUTION

Copies		CENTER DISTRIBUTION	
		Copies	Code
1	CNO/OP 980		
1	ONR/Code 470	1	17
1	NAVMAT/MAT 08T23	1	172
3	NRL	1	28
	1 Code 6300	10	281
	1 Code 6311	10	2814
	1 Code 6385	1	282
10	USNA	1	2821
9	NAVSEA	10	5214.1
	1 SEA 03	1	522.1
	1 SEA 03C	1	522.2
	1 SEA 035	2	5231
	1 SEA 08E		
	1 SEA 08S		
	1 SEA 09G32		
	1 SEA 924		
	1 PMS 393		
2	NAVSHIPYD		
	1 MARE		
	1 PTSMTH		
3	SUPSHIP		
	1 Groton		
	1 NPTNWS		
	1 Pascagoula		
10	NAVSEC		
	1 SEC 6034		
	1 SEC 6101		
	1 SEC 6105		
	1 SEC 6113		
	1 SEC 6114		
	2 SEC 6120D		
	1 SEC 6129		
	2 SEC 6129E		
12	DDC		

DTNSRDC ISSUES THREE TYPES OF REPORTS

1. DTNSRDC REPORTS, A FORMAL SERIES, CONTAIN INFORMATION OF PERMANENT TECHNICAL VALUE. THEY CARRY A CONSECUTIVE NUMERICAL IDENTIFICATION REGARDLESS OF THEIR CLASSIFICATION OR THE ORIGINATING DEPARTMENT.

2. DEPARTMENTAL REPORTS, A SEMI-FORMAL SERIES, CONTAIN INFORMATION OF A PRELIMINARY, TEMPORARY, OR PROPRIETARY NATURE OR OF LIMITED INTEREST OR SIGNIFICANCE. THEY CARRY A DEPARTMENTAL ALPHANUMERICAL IDENTIFICATION.

3. TECHNICAL MEMORANDA, AN INFORMAL SERIES, CONTAIN TECHNICAL DOCUMENTATION OF LIMITED USE AND INTEREST. THEY ARE PRIMARILY WORKING PAPERS INTENDED FOR INTERNAL USE. THEY CARRY AN IDENTIFYING NUMBER WHICH INDICATES THEIR TYPE AND THE NUMERICAL CODE OF THE ORIGINATING DEPARTMENT. ANY DISTRIBUTION OUTSIDE DTNSRDC MUST BE APPROVED BY THE HEAD OF THE ORIGINATING DEPARTMENT ON A CASE-BY-CASE BASIS.